# In Situ Studies of Methanol Decomposition and Oxidation on Pd(111) by PM-IRAS and XPS Spectroscopy

**ARTICLE** *in* THE JOURNAL OF PHYSICAL CHEMISTRY B · OCTOBER 2005

Impact Factor: 3.3 · DOI: 10.1021/jp053855c · Source: PubMed

THE JOURNAL OF PHYSICAL CHEMISTRY B LETTERS

**2005,** *109,* 17791−17794
Published on Web 08/31/2005



# In Situ Studies of Methanol Decomposition and Oxidation on Pd(111) by PM-IRAS and XPS Spectroscopy

**Marta Borasio, Oscar Rodríguez de la Fuente, Günther Rupprechter,* and Hans-Joachim Freund**

*Fritz-Haber-Institut der MPG, Faradayweg 4-6, D-14195 Berlin, Germany*

*Received: July 13, 2005; In Final Form: August 13, 2005*

Methanol decomposition and oxidation on Pd(111) at millibar pressure were studied by in situ polarization−modulation infrared reflection absorption spectroscopy (PM-IRAS), on-line gas chromatography and pre- and postreaction X-ray photoelectron spectroscopy (XPS). Various dehydrogenation products such as methoxy $CH_3O$, formaldehyde $CH_2O$, formyl CHO, and CO could be spectroscopically identified. Methanol oxidation proceeds via dehydrogenation to formaldehyde $CH_2O$, which either desorbs or is further dehydrogenated to CO, which is subsequently oxidized to $CO_2$. Carbonaceous overlayers that are present during the reaction may favorably affect the selectivity toward $CH_2O$. The reaction takes place on metallic Pd, and no indications of an involvement of Pd surface oxide were observed.

## Introduction

Methanol decomposition and oxidation on noble metal single crystals are prototypical reactions of surface science, because they serve as models for the interaction of alcohols or small organic molecules with catalysts (e.g., 1−9 and references therein). One has to keep in mind, however, that the adsorption/desorption conditions typically used for ultrahigh vacuum (UHV) studies are not necessarily representative for a catalytic reaction when the surface species are in equilibrium with the gas phase. In this letter, we present ambient (mbar) pressure studies of methanol oxidation and decomposition on Pd(111), employing a combination of in situ polarization−modulation infrared reflection absorption spectroscopy (PM-IRAS), on-line gas chromatography (GC), and pre- and postreaction X-ray photoelectron spectroscopy (XPS). It is shown that carbonaceous overlayers that are present during the reaction may not only act as poison but also increase the selectivity toward the partial oxidation product formaldehyde $CH_2O$ by blocking sites that are required for methanol dehydrogenation. XPS indicated that the reaction at 400−500 K took place on metallic Pd, i.e., no indications of Pd (surface) oxide were observed.

$CH_3OH$ dehydrogenation to CO and $H_2$ via O−H and C−H bond cleavage may provide a valuable source of syngas or hydrogen, provided that catalyst deactivation by carbon deposition via C−O bond scission can be suppressed.[10−14] It should be noted that it is critical to carry out these studies at elevated pressure. UHV studies of $CH_3OH$ decomposition indicated that desorption and dehydrogenation dominated and that Pd(111) was rather inactive for methanolic C−O bond scission ($CH_3OH$ mostly desorbed upon annealing before it reacted) (see, e.g., 1−6 and references therein). In contrast, already at $CH_3OH$ pressures of $>10^{-6}$ mbar, significant carbon deposition takes place, which cannot be neglected for a catalytic reaction.[8,9] It is therefore apparent that $CH_3OH$ oxidation also should be studied at elevated pressure. Methanol oxidation yields $CO_2$ and water as total oxidation products,[15] but the partial oxidation product formaldehyde $CH_2O$ is of higher value.

In this study, a Pd(111) single-crystal surface was used as well-defined model catalyst. Its surface structure and cleanliness were confirmed by low-energy electron diffraction (LEED) and XPS. The adsorption and reaction of gas molecules at millibar pressure were followed in situ by PM-IRAS. PM-IRAS makes use of the predominance of p- over s-polarized light at a metal surface and allows one to *simultaneously* acquire vibrational spectra of surface-adsorbed as well as gas-phase molecules. On-line GC was utilized to analyze and quantify the gas-phase composition to obtain turnover frequencies.

## Experimental Section

The experiments were carried out in a UHV surface analysis chamber combined with a UHV high-pressure reaction cell optimized for grazing incidence PM-IRAS.[16] The UHV section was equipped with LEED and XPS (Phoibos 150 using Mg Kα irradiation with a resolution of ∼1 eV). Pd(111) surfaces were prepared by sequences of ion bombardment, oxidation, and annealing as described in ref 17. The surface structure and cleanliness were confirmed by LEED and XPS, respectively, and were also indirectly examined by PM-IRAS using CO as the probe molecule. Only for clean, well-annealed Pd(111) does CO produce a perfect (2 × 2)-3CO structure, which exhibits a characteristic vibrational spectrum (with narrow peaks around 1895 and 2105 $cm^{-1}$).[17] Methanol (p.a.) was cleaned by repeated freeze−thaw cycles.

Quantitative analysis of XPS spectra (electron analyzer at a constant pass energy of 20 eV) was carried out by using the (2 × 2)-3CO saturation structure of CO on Pd(111) at 0.75 ML as reference (assuming identical sensitivity factors for CO,

* Corresponding author. G. Rupprechter, Fritz-Haber-Institut, Faradayweg 4-6, D-14195 Berlin, Germany. E-mail: rupprechter@fhi-berlin.mpg.de. Tel.: +49 30 8413 4132. Fax: +49 30 8413 4105.

10.1021/jp053855c CCC: $30.25 

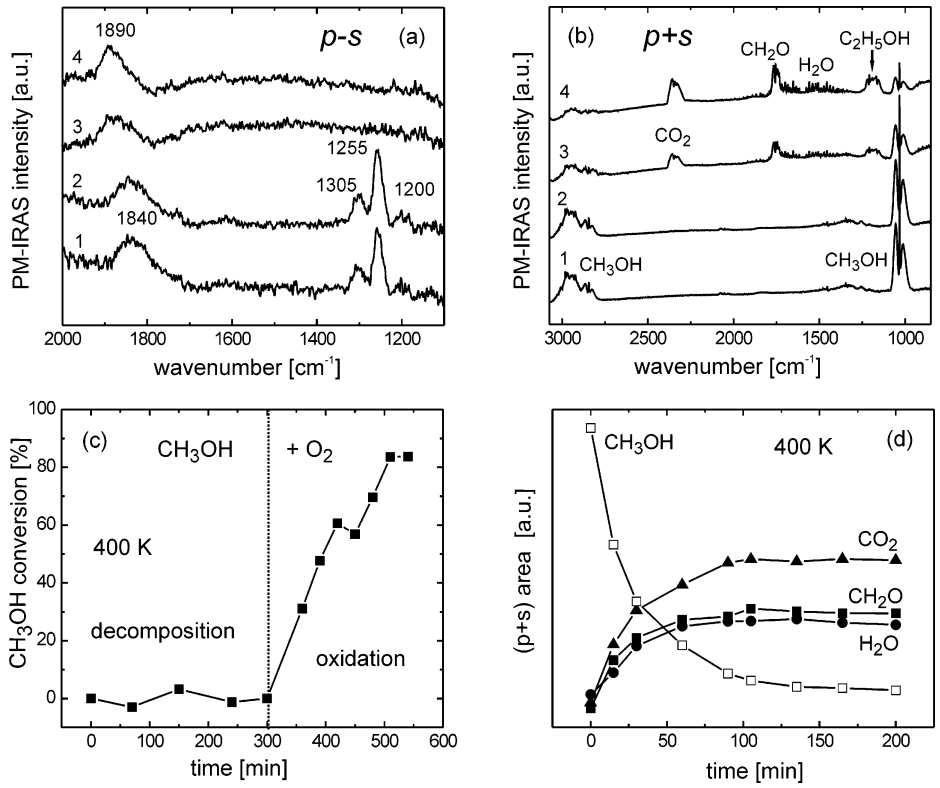


**Figure 1.** (a) Surface (p − s) and (b) gas-phase (p + s) PM-IRAS spectra measured during $CH_3OH$ oxidation at 300−400 K (5 mbar $CH_3OH$ added at 300 K (trace 1) prior to 5 mbar $O_2$ (trace 2)). Spectra 3 and 4 were acquired during the oxidation reaction at 400 K, after 15 and 60 min, respectively. Methanol conversion and formation of $CO_2$, $H_2O$, and $CH_2O$, as measured by gas chromatography and PM-IRAS (p + s), are displayed in (c) and (d), respectively.

$CH_xO$, and $CH_x$). Peak deconvolution was performed using the Levenberg−Marquardt method (standard nonlinear least-squares algorithm), using a mix of Gaussian and Lorentzian shapes and a tail function.

For PM-IRAS (Bruker IFS66v/S FTIR spectrometer, Hinds-PEM-90 photoelastic modulator), the sample was transferred under UHV to the high-pressure cell. To differentiate surface and gas-phase contributions, PM-IRAS makes use of the predominance of p- over s-polarized light at a metal surface, i.e., in p-polarization, both surface and gas-phase absorptions are detected, while in s-polarization, *only* the gas phase contributes to the signal. Accordingly, by polarization modulation of the incident infrared light and by monitoring the sum and difference interferograms, a surface vibrational spectrum $\Delta R/R = (R_p - R_s)/(R_p + R_s)$ is obtained. For further details about PM-IRAS, we refer to refs 16, 18, and 19.

## Results and Discussion

Figure 1a,b shows PM-IRAS surface (p − s) and gas-phase (p + s) spectra, respectively, acquired during methanol exposure and oxidation at millibar pressure. The gas-phase compositions, as determined by GC and PM-IRAS, are shown in Figure 1c and d, respectively (Figure 1d was obtained by integration of the gas-phase peaks in the (p + s) PM-IRAS spectra. The plotted lines only *qualitatively* show the disappearance/evolution of the different components because the peak areas were not calibrated. A quantitative analysis was performed by gas chromatography). After exposing 5 mbar $CH_3OH$ to Pd(111) at 300 K, PM-IRAS identified adsorbed CO ($\nu_{CO}$ at ∼1840 $cm^{-1}$, typical of ∼0.3 ML coverage) as well as formaldehyde ($\rho_{CH_2}$ of formaldehyde in two different adsorption geometries at 1305 and 1255 $cm^{-1}$ [20] (according to ref 20, formaldehyde is adsorbed in bridging and chelating geometry) and formyl CHO (CH bending or $\nu_{CO}$ at 1200 $cm^{-1}$ [20b]) (and minute amounts of methoxy around 2900 $cm^{-1}$; not shown; cf. Figure 3a). These species result from the dehydrogenation of methanol via methoxy, formaldehyde, and formyl to CO (Scheme 1).[21] Apart from these species, carbonaceous overlayers ($CH_x$) in excess of 1 ML were observed by in situ[9] and postreaction XPS. Hence, in the absence of oxygen, the surface is poisoned by CO, $CH_2O$, CHO, and $CH_x$. As a result, no activity for methanol decomposition was detected by GC analysis (Figure 1c), and also, corresponding PM-IRAS gas-phase spectra only detected the reactant $CH_3OH$ (Figure 1b, trace 1). One should note that under UHV conditions intermediate species of methanol decomposition were typically only observed at lower temperature. For instance, using HREELS, Davis and Barteau[22] observed formaldehyde species around 170 K, finally leading to adsorbed CO and hydrogen atoms on Pd(111) at ∼300 K. At 110 K, CHO was observed by Bhattacharya et al.[23] during $CH_3OH$ decomposition on Pd(110). Using IRAS, Barros et al.[20a] observed formaldehyde on Ru(0001) at 190 K.

**SCHEME 1: Illustration of $CH_3OH$ Decomposition and Oxidation on Pd(111), Including Only Those Species that Were Spectroscopically Detected**

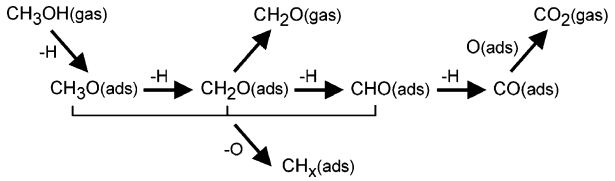


Upon oxygen addition, all surface species remained almost stable up to 350 K. The onset of catalytic activity was observed at 400 K, with $CH_2O$, $CO_2$, and $H_2O$ identified as gas-phase products by GC and PM-IRAS (p + s) spectra (Figure 1c,d). The $CH_3OH$ conversion after 3 h at 400 K was ∼84%, yielding

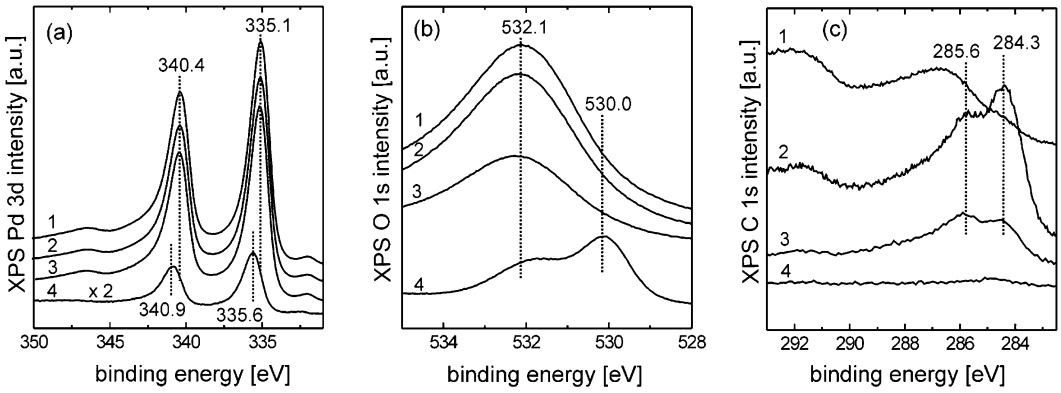


**Figure 2.** Pre- and postreaction XPS spectra in the Pd3d (a), O1s (b), and C1s (c) region: Pd(111) as prepared (trace 1, with a small amount of adsorbed CO); after the mbar reaction of Figure 1 at 400 K (trace 2); after mbar reaction at 500 K (trace 3). Reference measurements of Pd(111) oxidation at 650 K, yielding a Pd surface oxide, are also included (trace 4).

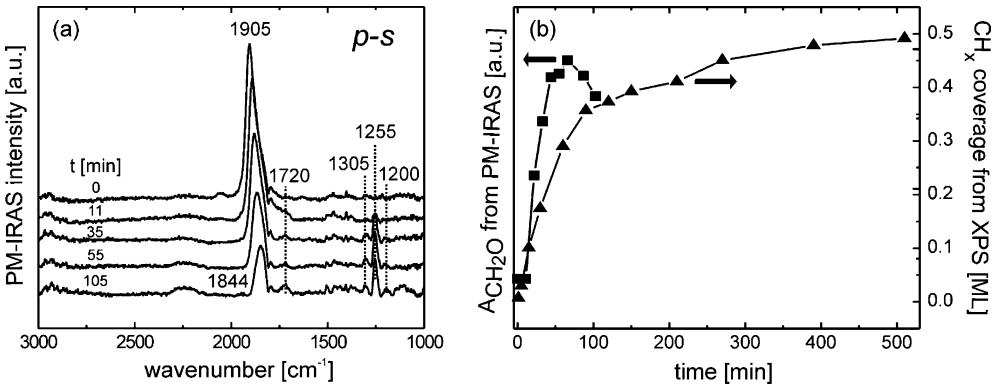


**Figure 3.** (a) PM-IRAS spectra (p − s) measured during $CH_3OH$ decomposition on Pd(111) at $\sim 10^{-5}$ mbar and 300 K. In (b), the time-dependent evolution of $CH_x$ (determined by XPS) and of $CH_2O$ (determined by PM-IRAS) are compared.

a turnover frequency of seven methanol molecules converted per Pd surface atom and second (initial turnover frequency of 15/site sec after 90 min of reaction) with a product distribution of ca. 10% $CH_2O$ and 25% $CO_2$ (GC and PM-IRAS also detected some ethanol and dimethyl ether, but this reaction path is not discussed here for conciseness). On the surface, PM-IRAS detected only CO, while formaldehyde and formyl had disappeared (Figure 1a, traces 3 and 4). Apparently, at 400 K, $CH_2O$ and CHO were reacted away, either by dehydrogenation to CO and/or by desorption. The amount of $CH_x$ under reaction conditions, as deduced from XPS, was 0.4 ML (Figure 2c, trace 2) (The peak at 284.3 eV is due to $CH_x$, that at 285.6 eV originates from CO. The two "bumps" in trace 1 (clean surface) are "Pd-satellites" due to the non-monochromated X-ray source and do not originate from adsorbed species). The reduced amount of $CH_2O$ and $CH_x$ under reaction conditions generated more free surface sites and led to a higher CO surface coverage, indicated by the shift of the CO peak to $\sim$1890 $cm^{-1}$ (typical of $\sim$0.4 ML CO) (Figure 1a, traces 3 and 4).

From these observations, we conclude that methanol oxidation proceeds via dehydrogenation to $CH_2O$, which either desorbs or is further dehydrogenated to CO, which is subsequently oxidized to $CO_2$ (Scheme 1). During the various dehydrogenation steps, reaction of hydrogen and oxygen produces, of course, water. Apparently, the surface concentration of $CH_2O$ (and CHO) is below the detection limit under reactive conditions.

It is now interesting to ask whether the $CH_x$ species that are present during the reaction were only undesired contaminants lowering the activity or whether $CH_x$ affected the reaction selectivity. For instance, $CH_x$ may favor $CH_2O$ formation by hindering its dehydrogenation to CO. One observation supporting this suggestion is that, at reaction temperatures of 500 K or higher, when the $CH_x$ concentration is much smaller (Figure 2c, trace 3), only $CO_2$ and water were observed as products in PM-IRAS (p + s) spectra (not shown). However, since this cannot prove an involvement of $CH_x$ in the oxidation reaction, we have also examined the time dependence of the evolution of $CH_x$ species and $CH_2O$. The formation of $CH_x$ is quite fast under millibar reaction conditions, and these experiments were therefore performed at reduced pressure.

Figure 3 compares PM-IRAS spectra and XPS data acquired during $\sim 10^{-5}$ mbar methanol exposure at 300 K. The (p − s) PM-IRAS spectrum in Figure 3a revealed CO as the only initial surface species with a coverage of $\sim$0.4 ML, in agreement with XPS. Under UHV conditions, methoxy, formaldehyde, and formyl are typically not observed at this temperature, which might be due to the absence of $CH_x$ species. However, at $\sim 10^{-5}$ mbar, PM-IRAS showed that formaldehyde and formyl surface species developed with time (peaks at 1255 and 1305 $cm^{-1}$ and at $\sim$1200 $cm^{-1}$, respectively) which are intermediate species of methanol dehydrogenation to CO. The growing peak around 1720 $cm^{-1}$ may be assigned to $\nu$(C−O) of a formyl species[20b] or to $\nu$(C−O) of formaldehyde[24] (its weak intensity suggests that $CH_2O$ is adsorbed with the C−O bond oriented (nearly) parallel to the surface). XPS cannot differentiate between CO and $CH_2O$ but indicated that the evolution of formaldehyde was paralleled by the evolution of $CH_x$ species (Figure 3b). According to a previous study,[9] $CH_x$ is most likely elemental carbon located in threefold hollow sites of Pd(111). However, $x$ may in fact be 0−3, because C−O bond scission could basically occur within methoxy, formaldehyde, and/or formyl, followed by further dehydrogenation (while no CO dissociation was observed[9]). Nevertheless, $CH_2O$ seems the most likely precursor for C−O bond cleavage due to its adsorption geometry.[16] A

comparison between the time-dependent evolution of $CH_2O$ (the relative amount was determined by integrating the PM-IRAS peaks at 1255 and 1305 $cm^{-1}$) and $CH_x$ is displayed in Figure 3b, which suggests that the formation of these species is in fact correlated. A possible explanation is that the carbon atoms prevent further dehydrogenation of formaldehyde to CO by poisoning the required (hollow) surface sites and/or by changing the electronic structure of neighboring Pd sites.[25] (Barros et al.[20a] reported that CO stabilized formaldehyde on Ru(0001), but an influence of $CH_x$ could not be excluded because no XPS was performed.) When the $CH_x$ coverage exceeded 0.4 ML, the $CH_2O$ signal was reduced because of significant surface poisoning. An involvement of the $CH_x$ species in steering the selectivity for methanol oxidation is thus very likely.

A final question concerns the state of the Pd(111) surface during the oxidation reaction at millibar pressure at 400 K (or higher). Surface oxides of Pd ($Pd_5O_4$ overlayer) and of other metals have recently raised much attention and may contribute to a reaction by supplying oxygen or by constituting the active phase.[26−30] In our study, postreaction XPS in the O1s region did not indicate any surface oxidation (Figure 2b, traces 2 and 3). The Pd3d region also only detected metallic Pd (Figure 2a, traces 2 and 3) but may not be sensitive enough, because we are probing ∼5−10 Pd layers and a possible oxidation of the first layer could be undetected. However, reference studies of Pd(111) oxidation at $10^{-5}$ mbar oxygen indicated the onset of surface oxidation at ∼600 K with clear shifts in the Pd3d and O1s lines,[29] as shown in Figure 2a,b (traces 4), respectively. Furthermore, the CO species observed during the oxidation reaction by PM-IRAS were typical of adsorption on *metallic* Pd. Consequently, the oxidation of the Pd surface, if present at all, must be minor.

**Acknowledgment.** Part of this work was supported by the German Science Foundation (DFG) through priority program SPP1091 (Ru 831/1-4). O.R.d.F. is grateful for a Humboldt fellowship.

## References and Notes

(1) Chen, J.-J.; Jiang, Z.-C.; Zhou, Y.; Chakraborty, B. R.; Winograd, N. *Surf. Sci.* **1995**, *328*, 248.
(2) Rebholz, M. M.; Kruse, N. *J. Chem. Phys.* **1991**, *95*, 7745.
(3) Mavrikakis, M.; Barteau, M. A. *J. Mol. Catal., A* **1998**, *131*, 135.
(4) Zhang, C. J.; Hu, P. *J. Chem. Phys.* **2001,** *115*, 7182.
(5) Desai, S. K.; Neurock, M.; Kourtakis, K. *J. Phys. Chem. B* **2002**, *106*, 2559.
(6) Schennach, R.; Eichler, A.; Rendulic, K. D. *J. Phys. Chem. B* **2003**, *107*, 2552.
(7) Hoffmann, J.; Schauermann, S.; Johánek, V.; Hartmann, J.; Libuda, J. *J. Catal.* **2003**, *213*, 176. Schauermann, S.; Hoffmann, J.; Johánek, V.; Hartmann, J.; Libuda, J.; Freund, H.-J. *Angew. Chem., Int. Ed.* **2002**, *41*, 2532.
(8) Rodríguez de la Fuente, O.; Borasio, M.; Galletto, P.; Rupprechter, G.; Freund, H.-J. *Surf. Sci.* **2004**, *740*, 566.
(9) Morkel, M.; Kaichev, V. V.; Rupprechter, G.; Freund, H.-J.; Prosvirin, I. P.; Bukhtiyarov, V. I. *J. Phys. Chem. B* **2004**, *108*, 12955.
(10) Wickham, D. T.; Logsdon, B. W.; Cowley, S. W.; Butler, C. D. *J. Catal.* **1991**, *128*, 198.
(11) Matsumura, Y.; Okumura, M.; Usami, Y.; Kagawa, K.; Yamashita, H.; Anpo, M.; Haruta, M. *Catal. Lett.* **1997**, *44*, 189.
(12) Cubeiro, M. L.; Fierro, J. L. G. *J. Catal.* **1998**, *179*, 150.
(13) Usami, Y.; Kagawa, K.; Kawazoe, M.; Matsumura, Y.; Sakurai, H.; Haruta, M. *Appl. Catal., A* **1998**, *General 171*, 123.
(14) Shiozaki, R.; Hayakawa, T.; Liu, Y. Y.; Ishii, T.; Kumagai, M.; Hamakawa, S.; Suzuki, K.; Itoh, T.; Shishido, T.; Takehira, K. *Catal. Lett.* **1999**, *58*, 131.
(15) Cordi, E. M.; Falconer, J. L. *J. Catal.* **1996**, *162*, 104.
(16) Rupprechter, G. *Annu. Rep. Prog. Chem., Sect. C* **2004**, *100*, 237.
(17) Morkel, M.; Rupprechter, G.; Freund, H.-J. *J. Chem. Phys.* **2003**, *119*, 10853.
(18) Beitel, G. A.; Laskov, A.; Oosterbeek, H.; Kuipers, E. W. *J. Phys. Chem.* **1996**, *100*, 12494.
(19) (a) Jugnet, Y.; Cadete Santos Aires, F. J.; Deranlot, C.; Piccolo, L.; Bertolini, J. C. *Surf. Sci.* **2002**, *521*, L639. (b) Ozensoy, E.; Hess, C.; Goodman, D. W. *J. Am. Chem. Soc.* **2002**, *124*, 8524.
(20) (a) Barros, R. B.; Garcia, A. R.; Ilharco, L. M. *J. Phys. Chem. B* **2001**, *105*, 11186. (b) Mitchell, W. J.; Xie, J.; Jachimowski, T. A.; Weinberg, W. H. *J. Am. Chem. Soc.* **1995**, *117*, 2606.
(21) Kruse, N.; Rebholz, M.; Matolin, V.; Chuah, G. K.; Block, J. H. *Surf. Sci. Lett.* **1990**, *238*, L457.
(22) Davis, J. L.; Barteau, M. A. *Surf. Sci.* **1990**, *235*, 235.
(23) Bhattacharya, A. K.; Chesters, M. A.; Pemble, M. E.; Sheppard, N. *Surf. Sci. Lett.* **1988**, *206*, L845.
(24) Davis, J. L.; Barteau, M. A. *J. Am. Chem. Soc.* **1989**, *111*, 1782.
(25) Stolbov, S.; Mehmood, F.; Rahman, T. S.; Alatalo, M.; Makkonen, I.; Salo, P. *Phys. Rev. B* **2004**, *70*, 155410.
(26) Leisenberger, F. P.; Koller, G.; Sock, M.; Surnev, S.; Ramsey, M. G.; Netzer, F. P.; Klötzer, B.; Hayek, K. *Surf. Sci.* **2000**, *445*, 380.
(27) Over, H.; Kim, Y. D.; Seitsonen, A. P.; Wendt, S.; Lundgren, E.; Schmid, M.; Varga, P.; Morgante, A.; Ertl, G. *Science* **2000**, *287*, 1474.
(28) Reuter, K.; Scheffler, M. *Phys. Rev. B* **2001**, *65*, 406.
(29) Lundgren, E.; Kresse, G.; Klein, C.; Borg, M.; Andersen, J. N.; De Santis, M.; Gauthier, Y.; Konvicka, C.; Schmid, M.; Varga, P. *Phys. Rev. Lett.* **2002**, *88*, 246103.
(30) Lundgren, E.; Gustafson, J.; Mikkelsen, A.; Andersen, J. N.; Stierle, A.; Dosch, H.; Todorova, M.; Rogal, J.; Reuter, K.; Scheffler, M. *Phys. Rev. Lett.* **2004**, *92*, 046101.